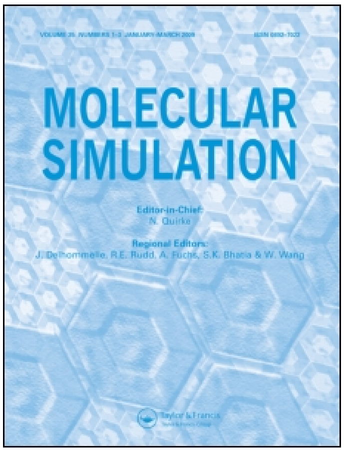

Molecular Simulation
Publication details, including instructions for authors and subscription information:
http://www.informaworld.com/smpp/title~content=t713644482

Quantum mechanics study on the selectivity of alkali metal cations by a novel fluorescent chemosensor

J. -W. Shen[a]; T. Wu[a]; Y. -G. Wang[a]; Q. Wang[a]
[a] Department of Chemistry, Zhejiang University, Hangzhou, People's Republic of China

To cite this Article Shen, J. -W. , Wu, T. , Wang, Y. -G. and Wang, Q.(2006) 'Quantum mechanics study on the selectivity of alkali metal cations by a novel fluorescent chemosensor', Molecular Simulation, 32: 14, 1123 — 1129

To link to this Article: DOI: 10.1080/08927020601007520

URL: http://dx.doi.org/10.1080/08927020601007520

Molecular Simulation, Vol. 32, No. 14, 15 December 2006, 1123–1129

Taylor & Francis
Taylor & Francis Group

Quantum mechanics study on the selectivity of alkali metal cations by a novel fluorescent chemosensor

J.-W. SHEN, T. WU, Y.-G. WANG and Q. WANG*

Department of Chemistry, Zhejiang University, Hangzhou 310027, People's Republic of China

(Received May 2006; in final form September 2006)

The selectivity of alkali metal cations (Na^+ and K^+) by a novel fluorescent chemosensor was investigated by quantum mechanics calculations. The binding energy calculations of the cationic complexes indicate that both of the aza-18-crown-6 rings bind Na^+ more strongly than K^+ and ring A favors both of Na^+ and K^+ comparing to ring B. The order of the stability implied by Gibbs free energy study agrees with that by binding energy calculation. Solvent effect was further investigated. Due to the large difference of solvation energies, the order of the stability of complexes changes in water.

Keywords: Chemosensor; Two-photon materials; Binding energy; Gibbs free energy change; Solvent effect

1. Introduction

Organic two-photon materials have received considerable interest due to their potential applications in three-dimensional optical storage [1,2], two-photon upconverted lasing [3,4], photodynamic therapy [5], and two-photon fluorescence excitation microscopy [6–8]. Two-photon laser scanning microscopy (TPLSM) is a powerful tool for three-dimensional imaging in biological systems, and it has been used to image the distribution of metal ions in living tissues [9,10]. Therefore, there are many researches on the selectivity and structure/property relationships for two-photon absorption [11–14]. Due to the selectivity of macrocycles, various fluoroionophores consisting of fluorophores linked to crown ether or azacrown ether are good candidates for the two-photon absorption. Thus, the structure/property relationships of these systems attract lots of attention [15–17]. For example, recently Pond *et al.* [18] reported the synthesis of mono- and bis-(aza-15-crown-5-ether) substituted donor-acceptor-donor distyrylbenzenes. They investigated the influence of metal cation's one- and two-photon spectroscopic properties, which is useful to the design of better two-photon excitable metal–ion sensing fluorophores.

In the past decades, crown ether and its derivatives were investigated as a chemosensor in various fields, especially for the efficient detection of important metal ionic species in biological and environmental sciences [19]. Theoretical calculations have been proved to be a powerful tool to design fluorescent chemosensors and provide better understanding of the conformations and ion selectivity for crown ether and its derivatives [20–31].

However, only few theoretical studies have been conducted on the structure/property of azacrown ether, especially for the two-azacrown ether systems. For example, Freidzon *et al.* [28] studied the photoinduced recoordination of Ca^{2+} complexes of photocheomic azacrown ethers by density functional method. They indicated that the presence of three or four water molecules in the coordination sphere of the cation decreases relative energies of the conformations with broken metal–nitrongen bond, thus favoring metal recoordination. Nevertheless, the absence of good understanding of structure/property for the two-azacrown ether systems limited our ability to design better organic two-photon materials. Recently, Hua *et al.* [32] synthesized a novel fluorescent chemosensor, denoted as chemosensor 1 later on, in which two aza-18-crown-6 moieties are linked to a coumarin fluorophore (figure 1 gives the structure of the chemosensor 1). It provides a good candidate for two-photon material application. However, the pure crystal of chemosensor 1 has not been derived. Hence, the ions-selective response of the fluorescence spectra of background metal ions (Na^+, K^+, Mg^{2+}, etc.) is not so reliable in that view. Theoretical investigation of this compound can help us to set up an ideal chemosensor-ions model to

---

*Corresponding author. Fax: + 86-571-8795-1895. Email: qiwang@zju.edu.cn

Molecular Simulation
ISSN 0892-7022 print/ISSN 1029-0435 online © 2006 Taylor & Francis
http://www.tandf.co.uk/journals
DOI: 10.1080/08927020601007520

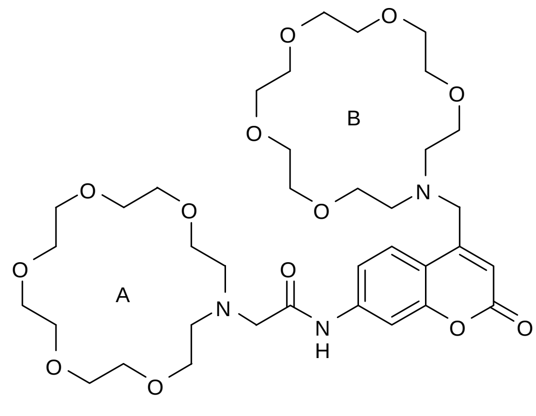

Figure 1. Structure of the chemosensor 1.

understand the structure/property relationships for two-photon absorption and to design better chemosensors which are available in ion recognition in biological and physiological conditions.

In this work, the selectivity of alkali metal cations (Na^+ and K^+) by the two aza-18-crown-6 rings of Hua's chemosensor was studied by quantum mechanics due to the physiological importance of Na^+ and K^+. All possible binding forms of chemosensor 1 and Na^+, K^+ were studied by binding energy, ΔE, and Gibbs free energy change, ΔG. The solvent effect was further studied by Onsager reaction field model.

2. Calculation methods

The free state of Chemosensor 1 and all the possible complexed forms, 2–9, are shown in table 1. Two aza-18-crown-6 rings were denoted as rings A and B, respectively. The complexation process of alkali metal cations and chemosensor 1 can be expressed by following equations:

$$M^+ + \text{chemosensor 1} \longrightarrow M_A^+(\text{chemosensor 1}) \quad (1)$$

$$\text{or } M^+ + \text{chemosensor 1} \longrightarrow (\text{chemosensor 1})M_B^+ \quad (2)$$

$$\text{or } M_1^+ + M_2^+ + \text{chemosensor 1} \longrightarrow M_{1A}^+(\text{chemosensor 1})M_{2B}^+ \quad (3)$$

where M stands for alkali metal cations (K^+ or Na^+).

Semi-empirical AM1 method has been applied successfully to the geometry optimization of Li^+-1,10-diaza-18-crown-6 complexes [33]. Considering the size of the aimed systems and the balance between the accuracy and the computing expense, all the geometric optimizations of free chemosensor and cationic complexes were performed at the AM1 level of theory with HyperChem 7.0. The frequencies were also calculated on the optimized geometries in order to confirm whether these geometries correspond to energy minima.

Single point energy calculation were further performed by Gaussian 03 [34] on the optimized geometries at the B3LYP/6-31G* level of theory. The binding energy can be expressed as:

$$E_{\text{binding}} = E_{\text{complex}} - E_{\text{donor}} - E_{\text{acceptor}} \quad (4)$$

where E_{complex} is the total energy of different cationic complexes, E_{donor} is the total energy of the free chemosensor 1, and E_{acceptor} is the total energy of alkali metal cation. The binding energy in solvent can also be expressed by equation (4) if the total energy of complex, donor and acceptor in solvent are calculated. The solvation energies were also calculated in Gaussian 03 with Onsager reaction field model [35].

In equation (4), only the enthalpies were taken into consideration but not entropies. Hence the Gibbs free energy change, which takes the entropy effect into account, was further calculated by:

$$\begin{aligned}\Delta G &= G_{\text{complex}} - G_0 \\ &= H_{\text{complex}} - TS_{\text{complex}} - (H_0 - TS_0) \\ &= \Delta H - T\Delta S \qquad (5)\end{aligned}$$

where G_{complex}, H_{complex} and S_{complex} stand for the Gibbs free energy, enthalpy and entropy of complexes, respectively, and G_0, H_0 and S_0 stand for the Gibbs free energy, enthalpy and entropy of free chemosensor 1.

3. Result and discussion

3.1 Structure

Geometric optimization of free chemosensor 1 was conducted at AM1 level of theory. Figure 2 shows the optimized geometry of chemosensor 1. As the crown ether derivative has two flexible rings, the conformations of the cationic complexes differ significantly from the original one. The sizes of the two aza-18-crown-6 cavities increase when two rings bind K^+ or Na^+. Figure 3 shows the geometries of different cationic complexes. The Electrostatic interaction of the cation with the crown ether backbone is one of the most important factors that affect the binding affinity of crown ether. The information about the M^+–O and M^+–N distances of two rings of optimized

Table 1. Eight possible binding forms of chemosensor 1 with Na^+, K^+.

	1	*2*	*3*	*4*	*5*	*6*	*7*	*8*	*9*
Ring A				K^+	Na^+	K^+	Na^+	K^+	Na^+
Ring B		K^+	Na^+			K^+	Na^+	Na^+	K^+

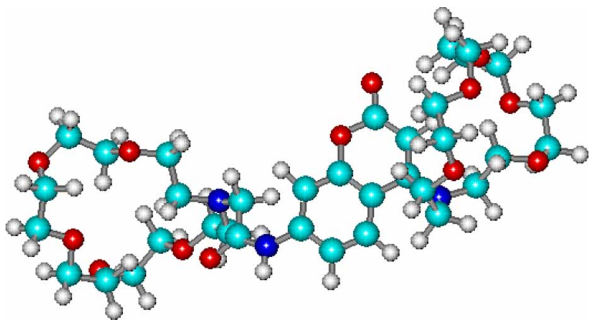

Figure 2. Geometry of the chemosensor 1 optimized at the AM1 level.

cationic complexes is listed in table 2. For ring A, the mean K^+–O distances of cationic complexes 4, 6 and 8 are all 2.80 Å. If change K^+ to Na^+ in ring A (cationic complexes 5, 9 and 7), all the corresponding mean Na^+–O distances are 0.09 Å shorter than that of K^+–O. But the K^+–N distance of those cationic complexes are 4.11, 3.53 and 3.53 Å, which is 0.02, 0.58 and 0.60 Å shorter than the corresponding Na^+–N distances, respectively. As to ring B, the mean K^+–O distances of cationic complexes 2, 6 and 9 are 3.02, 3.01 and 3.01 Å. The corresponding mean Na^+–O distances (cationic complexes 3, 8 and 7) are 0.02, 0.02 and 0.01 Å longer than the mean K^+–O distances. But the K^+–N distances of those cationic complexes are 3.52, 3.53 and 3.53 Å, respectively, about 0.20 Å longer than their corresponding Na^+–N distances. It suggests that, in ring A, the electrostatic interaction of K^+ with N atom is stronger than that of Na^+ with N atom, while the electrostatic interaction between Na^+ and O atoms is stronger than that of K^+ and O atoms. Nevertheless, the phenomenon observed in ring B is reversed, in which the electrostatic interaction of Na^+ with N atom is stronger than that of K^+ with N atom, but the electrostatic

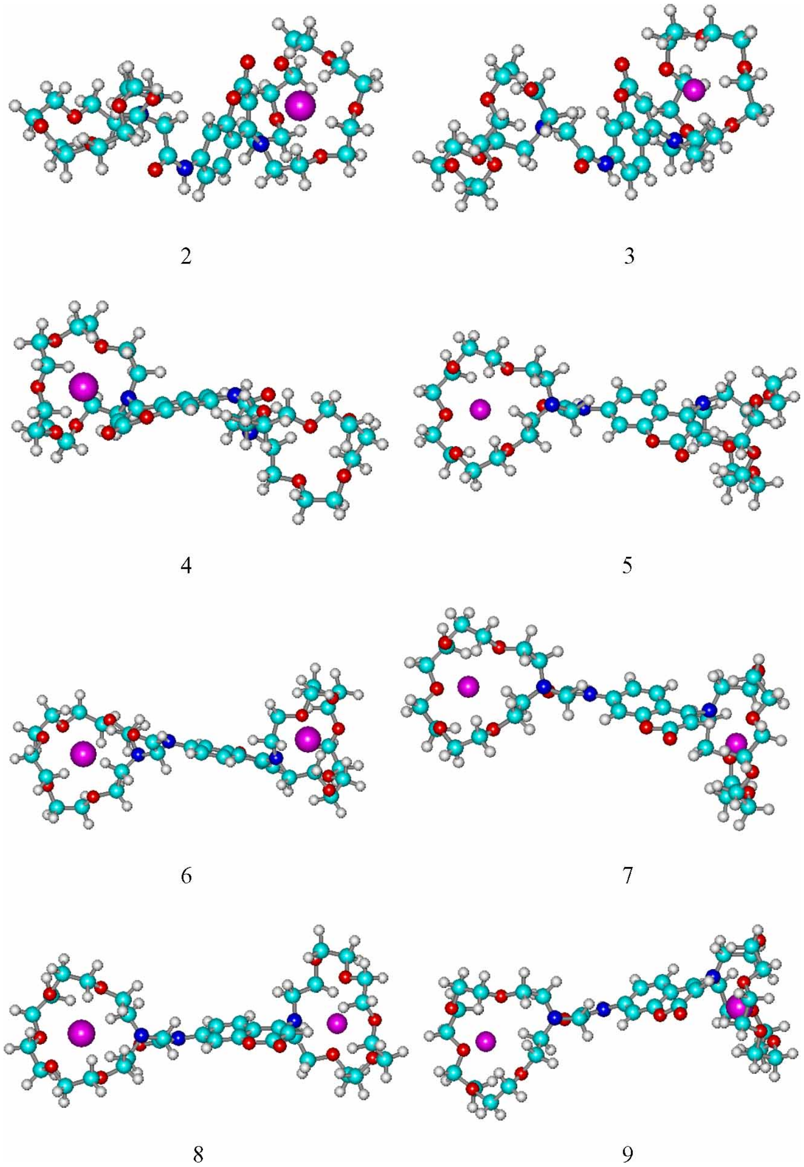

2 3

4 5

6 7

8 9

Figure 3. Geometry of eight cationic complexes optimized at the AM1 level.

Table 2. M–O and M–N distances of two rings of optimized cationic complexes.

	Ring A				*Ring B*			
	M–O distances (Å)				*M–O distances (Å)*			
Complexes	*Min*	*Mean*	*Max*	*M–N distances (Å)*	*Min*	*Mean*	*Max*	*M–N distances (Å)*
2					2.78	3.02	3.90	2.78
3					2.71	3.04	4.20	2.59
4	2.74	2.80	2.87	4.11				
5	2.64	2.71	2.77	4.12				
6	2.77	2.80	2.83	3.53	2.77	3.01	3.88	2.78
7	2.64	2.71	2.75	4.13	2.70	3.02	4.17	2.61
8	2.76	2.80	2.84	3.53	2.71	3.03	4.16	2.56
9	2.63	2.71	2.75	4.11	2.78	3.01	3.88	2.78

interaction of K^+ with O atoms is stronger than that of Na^+ with O atoms.

3.2 Binding energy

In order to explore the effect of the size of basis set on the binding energy, a variety of basis sets were carried out on the optimized free chemosensor 1. The total energy of the free chemosensor 1 decreases as the basis set increases. As the basis set increase from STO-3G to 6-31G*, the total energy of the free chemosensor 1 calculated by both RHF and B3LYP decreases remarkably. The energy differences of 6-31G* and 6-31G** basis set using both of the RHF and B3LYP methods are relatively small (0.0920 hartrees for RHF and 0.0766 hartrees for B3LYP). Considered the balance of expense and precision, the basis set 6-31G* was employed for single point energy calculation. Due to the advantages of describing electronic correlation, the total energy of B3LYP calculation is 15.0958 Hatrees lower than that of RHF calculation at the 6-31G* level of theory. The B3LYP/6-31G* set was finally selected for all the single point energy calculations of the free chemosensor 1 and its complexes.

The total energy (E) and the binding energy (ΔE) of free and complexed chemosensor 1 were calculated. The alkali metal selectivity of two aza-18-crown-6 rings deduced from binding energy was presented in figure 4. The binding energies of these complexes range from 78.3 to 433.7 kJ/mol. For cationic complexes 4 and 5, ring A complexes with K^+ and Na^+, respectively. The binding energy of cationic complex 5 is 127.9 kJ/mol smaller than that of cationic complex 4. It indicates that ring A binds Na^+ more strongly than K^+ when ring B is empty. For cationic complexes 7 and 8, both of the ring B complex with Na^+, but ring A complex with Na^+ and K^+, respectively. We considered that cations selection occurs after aza-18-crown-6 ring B complex with Na^+. So ring A binds Na^+ 141.4 kJ/mol more strongly than K^+ in that case. It is similar for cationic complexes 6 and 9: ring A binds Na^+ 154.6 kJ/mol more strongly than K^+ when ring B complexed with K^+. The selectivity of alkali metal cations of aza-18-crown-6 ring B is similar to that of aza-18-crown-6 ring A. The binding energy of cationic complex 3 is 171.9 kJ/mol smaller than that of cationic complex 2. It reveals that ring B also binds Na^+ more strongly than K^+ when ring A is empty. In the case that ring A complex with Na^+ or K^+, ring B favor Na^+ 151.5 kJ/mol or 164.8 kJ/mol. The selectivity of Na^+ and K^+ by both of the aza-18-crown-6 rings is as same as that by 18-crown-6 in Glendening's report [31] judging from binding energy. However, the binding energy of Na^+ by 18-crown-6 is a little larger than that by both of the aza-18-crown-6 rings, while the difference of binding energy for K^+ with 18-crown-6 and two aza-18-crown-6 rings is more than 100 kJ/mol. It reveals the weak selectivity of K^+ by two aza-18-crown-6 rings. By contrasting cationic complexes 3 and 5, 2 and 4, it can be found that ring A binds Na^+ 37.1 kJ/mol more strongly than ring B, and binds K^+ 81.1 kJ/mol more strongly than ring B. Another interesting finding is that if ring B binds an cation (Na^+ or K^+), chemosensor 1 will be more stable in the case that ring A binds another cation. For example, the binding energy of cationic complex 8 is 42.2 kJ/mol lower than cationic complex 3. Similarly, if an cation (Na^+ or K^+) occupy ring A first, binding Na^+ by ring B also stabilize the cationic complexes. However, in this case, binding K^+ by ring B causes the cationic complexes a little unstable. For example, the binding energy of complex 4 is 31.8 kJ/mol lower than that of complex 6, and the binding energy of complex 5 is 5.1 kJ/mol lower than that of complex 9. These phenomena also suggest the stronger interaction between Na^+ and ring B comparing with the interaction between K^+ and ring B.

Table 3. Enthalpies, entropies and gibbs free energy changes of eight cationic complexes in 300 K.

Complexes	*ΔH (kJ/mol)*	*ΔS (J/mol.K)*	*ΔG (kJ/mol)*
2	−75.6	15.1	−80.2
3	−245.4	67.0	−265.5
4	−157.5	−8.9	−154.9
5	−283.8	12.0	−287.4
6	−123.3	−5.9	−121.5
7	−426.4	35.3	−436.9
8	−286.5	9.4	−289.3
9	−276.2	21.3	−282.6

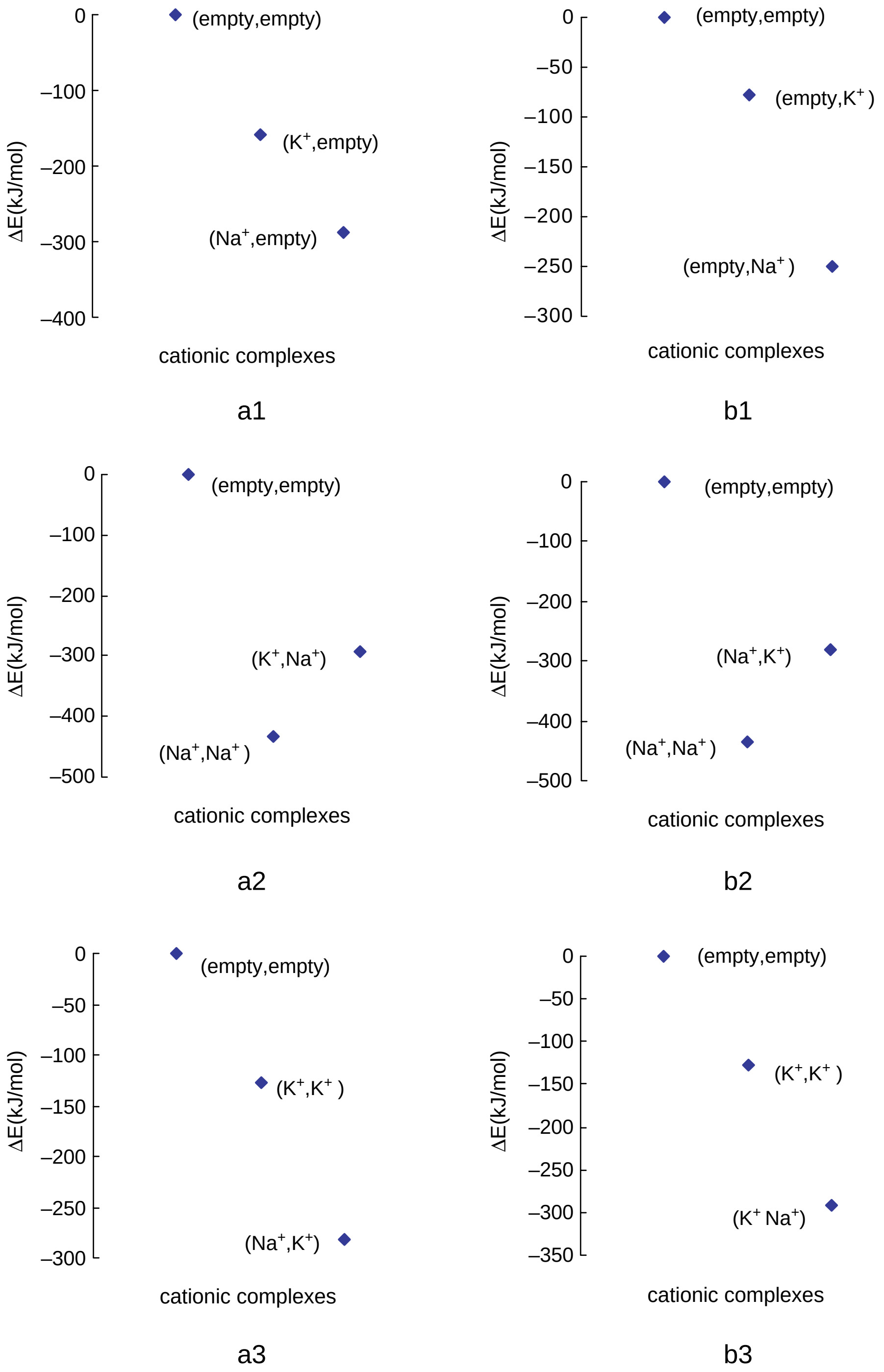

Figure 4. Alkali metal cation selectivity of aza-18-crown-6 rings A and B based on binding energy. Cations at the left of the parentheses complex with ring A and cations at the right of the parentheses complex with ring B. Empty means no alkali metal cations complex with aza-18-crown-6 ring.

3.3 Gibbs free energy change

Since conformations of the cationic complexes differ significantly from the free chemosensor 1, the thermodynamic functions including entropy were calculated. The values of enthalpy, entropy and Gibbs free energy change of all cationic complexes in 300 K were listed in table 3. The contribution of entropy changes ($T\Delta S$) to the free energy changes of all cationic complexes in 300 K is from -2.7 to 20.1 kJ/mol. The percents of entropy changes to the ΔH of corresponding cationic complexes range from 0.99 to 8.19%. It illustrated that the entropy change is a small percentage of the Gibbs free energy change in the complexation of chemosensor 1 and alkali metal cations (Na^+ and K^+), and the entropy change is not as important as the enthalpy change during the complexation. Clear views of ΔH, ΔG and $-T\Delta S$ at 300 K are shown in figure 5.

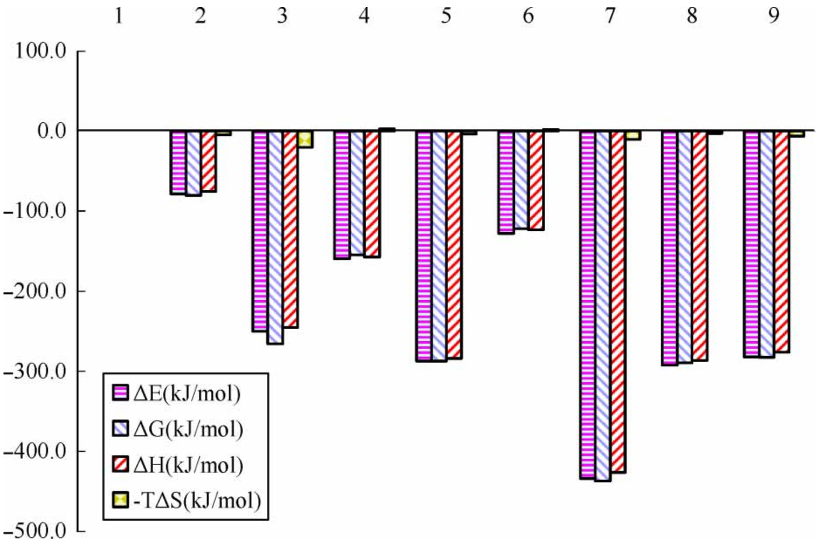

Figure 5. ΔE and ΔH, $-T\Delta S$, ΔG of cationic complexes in 300 K.

The order of the stability implied by Gibbs free energy study agrees with that by binding energy calculation. Figure 5 also shows the binding energies and Gibbs free energy changes of the cationic complexes. Gibbs free energy changes are very close to the binding energies due to the relatively small entropy changes during the complexation. In the cases that aza-18-crown-6 ring B binds nothing, Na^+ or K^+, the values of ΔG of the complexation of Na^+ by ring A are 132.6, 147.6 and 161.0 kJ/mol smaller than ΔG of the complexation of K^+ by ring A. Ring B also exhibits the selectivity of Na^+ contrast to K^+.

3.4 Solvent effect

The solvent effect of these cationic complexes was also examined. But unfor- tunately, all the calculations using both of the polarizable continuum model (PCM) and the Conductor-like Screening Model failed to converge. Finally, Onsager reaction field model was employed to get the converged results. The energy calculations were taken under the B3LYP/6-31G* level of theory. The total energies (E'), solvation energies (E_S) and binding energies ($\Delta E'$) of eight cationic complexes in water are listed in table 4. If the binding energies in water were examined in the same way as that in gas phase, it is easy to find that both rings A and B bind Na^+ more strongly than K^+. However, due to the solvent effect, the order of the stability of complexes that bind one cation and two cations changes in water. The solvation energies of complexes 2–5 which bind only one cation (from 83.2 to 117.9 kJ/mol), is much larger than that of complexes 6–9 (from 3.9 to 11.6 kJ/mol) which bind two cations. For example, the bind energy of complex 2 is 49.3 kJ/mol higher than complex 6 in gas phase, but it is 22.3 kJ/mol lower than complex 6 in water due to its relatively large solvation energy. Similarly, the relative stability of complexes 3 and 8 is reverse in gas phase and in water. It clearly shows that in water when either of the two rings binds a cation (Na^+ or K^+) it is difficulty to bind K^+ by another ring. Whereas, the chemosensor 1 could selectively bind Na^+ as long as it has a free ring owing to the strong interaction between two rings and Na^+.

Table 4. Total energies (E'), solvation energies (E_S) and binding energies ($\Delta E'$) of eight cationic complexes in water (B3LYP/6-31G* values).

Complexes	E' *(hartree)*	E_S *(kJ/mol)*	$\Delta E'$ *(kJ/mol)*
1(free)	− 2508.79017	1.6	
2	− 3108.57604	83.2	− 159.9
3	− 2670.99824	84.4	− 333.0
4	− 3108.62018	117.9	− 275.7
5	− 2671.02511	117.9	− 403.6
6	− 3708.29254	11.6	− 137.6
7	− 2833.11987	7.0	− 439.1
8	− 3270.70896	4.8	− 295.6
9	− 3270.70472	3.9	− 284.4

4. Conclusion

A quantum mechanics study of the complexation of alkali metal cations Na^+ and K^+ by both aza-18-crown-6 rings of a novel fluorescent chemosensor was presented. Geometries of all possible forms of cationic complexes were optimized. The optimized geometries differ significantly from the optimized free chemosensor 1 due to the flexibility of crown ether backbones. The interactions of alkali metal cations with N and O atoms were investigated. *Ab initio* study reveals that both of the aza-18-crown-6 rings bind Na^+ more strongly than K^+. In addition, ring A bind two cations more strongly than ring B. The result of the Gibbs free energy calculation agrees with the binding energy study, which is attributed to the relatively small entropy changes (maximum 20.1 kJ/mol) during the complexation. It indicates that entropy effect is not as important as the enthalpy effect during the complexation. Gibbs free energy changes also shows that two rings favor

Na^+ compared with K^+ and ring A bind two cations more strongly than ring B. All of our work shows that both of the aza-18-crown-6 rings preferentially bind the small alkali metal cations (Na^+) both in gas phase and in water. However, the order of the stability is partly changed if the solvent effect was taken into consideration. To understand the behavior of the chemosensor in different solvents more clearly, further investigation by molecular dynamics, which use the force field derived from the present calculations, is still undergoing.

Acknowledgements

This work was financially supported by the National Natural Science Foundation of China (Grant No. 20503025 and No. 60533050).

References

[1] D.A. Parthenopoulos, P.M. Rentzepis. Three-dimensional optical storage memory. *Science*, **245**, 843 (1989).

[2] B.H. Cumpston, S.P. Ananthavel, S. Barlow, D.L. Dyer, J.E. Ehrlich, L.L. Erskine, A.A. Heikal, S.M. Kuebler, I.-Y.S. Lee, D. McCordMaughon, J. Qin, H. Röckel, M. Rumi, X.L. Wu, S.R. Marder, J.W. Perry. Two-photon polymerization initiators for three-dimensional optical data storage and microfabrication. *Nature*, **398**, 51 (1999).

[3] C.F. Zhao, G.S. He, J.D. Bhawalkar, C.K. Park, P.N. Prasad. Newly synthesized dyes and their polymer/glass composites for one- and two-photo pumped solid-state cavity lasing. *Chem. Mater.*, **7**, 1979 (1995).

[4] G.S. He, C.F. Zhao, J.D. Bhawalkar, P.N. Prasad. Two-photon pumped cavity lasing in novel dye doped bulk matrix rods. *Appl. Phys. Lett.*, **67**, 3703 (1995).

[5] J.D. Bhawalkar, N.D. Kumar, C.F. Zhao, P.N. Prasad. Two-photon photodynamic therapy. *J. Clin. Laser Med. Surg.*, **15**, 201 (1997).

[6] W. Denk, J.H. Strickler, W.W. Webb. Two-photon laser scanning fluorescence microscopy. *Science*, **248**, 73 (1990).

[7] R.H. Köhler, J. Cao, W.R. Zipfel, W.W. Webb, M.R. Hansen. Exchange of protein molecules through connections between higher plant plastids. *Science*, **276**, 2039 (1997).

[8] W. Denk, K. Svoboda. Photo upmanship: why multiphoto imaging is more than a gimmick. *Neuron*, **18**, 351 (1997).

[9] C. Stosiek, O. Garaschuk, K. Holthoff, A. Konnerth. *In vivo* two-photon calcium imaging of neuronal networks. *Proc. Nat. Acad. Sci.*, **100**, 7319 (2003).

[10] M. Rubart, E.X. Wang, K.W. Dunn, L.J. Field. Two-photon molecular excitation imaging of Ca^{2+} transients in Langendorff-perfused mouse hearts. *Am. J. Physiol. Cell Physiol.*, **284**, C1654 (2003).

[11] M. Rumi, J.E. Ehrlich, A.A. Heika, J.W. Perry, S. Barlow, Z.Y. Hu, D. McCord-Maughon, T.C. Parker, H. Röckel, S. Thayumanavan, S.R. Marder, D. Beljonne, J.-L. Brédas. Structure-property relationships for two-photon absorbing chromophores: bis-donor diphenylpolyene and bis(styryl)benzene derivatives. *J. Am. Chem. Soc.*, **122**, 9500 (2000).

[12] B.R. Cho, K.H. Son, S.H. Lee, Y.-S. Song, Y.-K. Lee, S.-J. Jeon, J.H. Choi, H. Lee, M. Cho. Two photon absorption properties of 1,3,5-Tricyano-2,4,6-tris(styryl)benzene derivatives. *J. Am. Chem. Soc.*, **123**, 10039 (2001).

[13] W.-H. Lee, M. Cho, S.-J. Jeon, B.R. Cho. Two-photon absorption and second hyperpolarizability of the linear quadrupolar molecule. *J. Phys. Chem. A*, **104**, 11033 (2000).

[14] M. Taki, J.L. Wolford, T.V. O'Halloran. Emission ratiometric imaging of intracellular zinc: design of a benzoxazole fluorescent sensor and its application in two-photon microscopy. *J. Am. Chem. Soc.*, **126**, 712 (2004).

[15] V. Thanabal, V. Krishnan. Porphyrins with multiple crown ether voids: novel systems for cation complexation studies. *J. Am. Chem. Soc.*, **104**, 3643 (1982).

[16] P. Dumon, G. Jonusauskas, F. Dupuy, Ph. Pée, C. Rullière. Picosecond dynamics of cation-macrocycle interactions in the excited state of an intrinsic fluorescence probe: the calcium complex of 4-(*N*-Monoaza-15-crown-5)-4′-phenylstilbene. *J. Phys. Chem.*, **98**, 10391 (1994).

[17] H.M. Kim, M.-Y. Jeong, H.C. Ahn, S.-J. Jeon, B.R. Cho. Two-photon sensor for metal ions derived from azacrown ether. *J. Org. Chem.*, **69**, 5749 (2004).

[18] S.J.K. Pond, O. Tsutsumi, M. Rumi, O. Kwon, E. Zojer, J.-L. Brédas, S.R. Marder, J.W. Perry. Metal–ion sensing fluorophores with large two-photon absorption cross sections: aza-crown ether substituted donor-acceptor-donor distyrylbenzenes. *J. Am. Chem. Soc.*, **126**, 9291 (2004).

[19] G.W. Gokel, W.M. Leevy, M.E. Weber. Crown ethers: sensors for ions and molecular scaffolds for materials and biological models. *Chem. Rev.*, **104**, 2723 (2004).

[20] B.P. Hay, J.R. Rustad, C.J. Hostetler. Quantitative structure-stability relationship for potassium ion complexation by crown ethers. A molecular mechanics and *ab initio* study. *J. Am. Chem. Soc.*, **115**, 11158 (1993).

[21] T.P. Straatsma, J.A. McCammon. Treatment of rotational isomers in free energy calculations. II. Molecular dynamics simulation study of 18-crown-6 in aqueous solution as an example of systems with large numbers of rotational isomeric states. *J. Chem. Phys.*, **91**, 3631 (1989).

[22] Y. Sun, P.A. Kollman. Determination of solvation free energy using molecular dynamics with solute Cartesian mapping: an application to the solvation of 18-crown-6. *J. Chem. Phys.*, **97**, 5108 (1992).

[23] T. Kowall, A. Geiger. Molecular dynamics simulation study of 18-crown-6 in aqueous solution. 1. Structure and dynamics of the hydration shell. *J. Phys. Chem.*, **98**, 6216 (1994).

[24] T. Kowall, A. Geiger. Molecular dynamics simulation study of 18-crown-6 in aqueous solution. 2. Free energy profile for the association $18C6\cdots K^+$ in water. *J. Phys. Chem.*, **99**, 5240 (1995).

[25] A.A. Bagatur'yants, A.Ya. Freidzon, M.V. Alfimov, E.J. Baerends, J.A.K. Howard, L.G. Kuz'mina. DFT calculations on the electronic and geometrical structure of 18-crown-6 complexes with Ag^+, Hg^{2+}, Ag^0, Hg^+, Hg^0, $AgNO_3$, and HgX_2 ($X = Cl$, Br, and I). *J. Mol. Struct. (Theochem)*, **588**, 55 (2002).

[26] A.Ya. Freidzon, A.A. Bagatur'yants, S.P. Gromov, M.V. Alfimov. Recoordination of a metal ion in the cavity of a crown compound: a theoretical study. 1. Conformers of arylazacrown ethers and their complexes with Ca^{2+} cation. *Russ. Chem. Bull.*, **52**, 2646 (2003).

[27] A.Ya. Freidzon, A.A. Bagatur'yants, S.P. Gromov, M.V. Alfimov. Recoordination of a metal ion in the cavity of a crown compound: a theoretical study 2.* Effect of the metal ion-solvent interaction on the conformations of calcium complexes of arylazacrown ethers. *Russ. Chem. Bull.*, **54**, 2042 (2005).

[28] A.Ya. Freidzon, A.A. Bagatur'yants, S.P. Gromov, M.V. Alfimov. Recoordination of a metal ion in the cavity of an arylazacrown ether: model study of the conformations and microsolvation of calcium complexes of arylazacrown ethers. *Int. J. Quantum Chem.*, **100**, 617 (2004).

[29] H. Takemura, K. Sako. $Li^+\cdots\pi$ interaction in coronene-azacrown ether system. *Tetrahedron Lett.*, **46**, 8169 (2005).

[30] A.L. Sargent, B.J. Mosley, J.W. Sibert. A theoretical investigation on the wurster's crown analogue of 18-crown-6. *J. Phys. Chem. A*, **110**, 3826 (2006).

[31] E.D. Glendening, D. Feller, M.A. Thompson. An *ab initio* investigation of the structure and alkali metal cation selectivity of 18-crown-6. *J. Am. Chem. Soc.*, **116**, 10657 (1994).

[32] J. Hua, Y.G. Wang. A highly selective and sensitive fluorescent chemosensor for Fe^{3+} in physiological aqueous solution. *Chem. Lett.*, **34**, 98 (2005).

[33] Q.Z. Chen, K. Cannell, J. Nicoll, D.V. Dearden. The macrobicyclic cryptate effect in the gas phase. *J. Am. Chem. Soc.*, **118**, 6335 (1996).

[34] M.J. Frisch, et al. *Gaussian 03, Revision B.02*, Gaussian, Inc., Pittsburgh, PA (2003).

[35] L. Onsager. Electric moments of molecules in liquids. *J. Am. Chem. Soc.*, **58**, 1486 (1936).